Design of a Robust Voltage Controller for an Induction Generator in an Autonomous Power System Using a Genetic Algorithm

Vitaly Spitsa, Alon Kuperman, George Weiss *and* Raul Rabinovici

***Abstract*—We present a new voltage controller for an induction generator in an autonomous power system. The controller acts via a PWM inverter which is connected in parallel with the induction generator and maintains a constant voltage magnitude at the generator terminals. In addition to this voltage regulation, the controller successfully eliminates harmonic distortions caused by nonlinear loads. Unlike earlier controllers designed for such a system, our controller is not based on a hysteresis rule. It incorporates a finite dimensional internal model with adjustable resonant frequencies and a stabilizing compensator designed using genetic optimization combined with H^∞ design. The proposed controller can be implemented digitally with synchronous sampling. To examine the performance of this controller, computer simulations of a full power system model were carried out in Simulink®. The results show the advantages of the new voltage controller.**

***Index Terms*—AC generator excitation, Algorithms, Converters, Harmonic distortion, Uncertainty, Voltage control.**

I. Introduction

Increasing use of renewable energy sources has stimulated an intensive research to develop economically efficient methods of energy conversion. Many different power system configurations and control schemes were proposed for distributed power generation. Doubly-fed induction machines are often used as generators, for example in wind farms [1]. Squirrel-cage induction machines are cheaper, simpler and more robust, but more difficult to control. Sometimes they are also used as generators in autonomous power systems. To produce electrical energy, such generators must be excited from an external source of reactive power. A standard solution for this problem is to connect a capacitor bank in parallel with the induction generator [2]. However, this self-excited configuration suffers from very serious drawbacks: it is not possible to control the voltage and the frequency under non-constant load conditions. Therefore, any change of load power may result in large magnitude voltage transients and even instability. To overcome this disadvantage the capacitor bank is replaced by or supplemented with a controlled inverter called solid-state synchronous voltage source [3],[4]. Usually, the solid-state synchronous voltage source is implemented as a voltage source inverter (VSI) since modern PWM techniques are more suitable for this [4].

In this work we present a voltage controller design for the autonomous power system shown in Fig. 1. Here, IG is a squirrel-cage induction generator. Its excitation system consists of a VSI connected in parallel with a capacitor bank to decrease the rated power of the VSI. The proposed controller allows us to retain a prescribed magnitude of the three-phase balanced sinusoidal voltages at the generator terminals in spite of load variations, prime mover speed fluctuations and harmonic disturbance from the non-linear loads. This controller can be found using a genetic algorithm for parameter optimization of an H^∞ problem with additional criteria and incorporates an internal model with adjustable resonance frequencies.

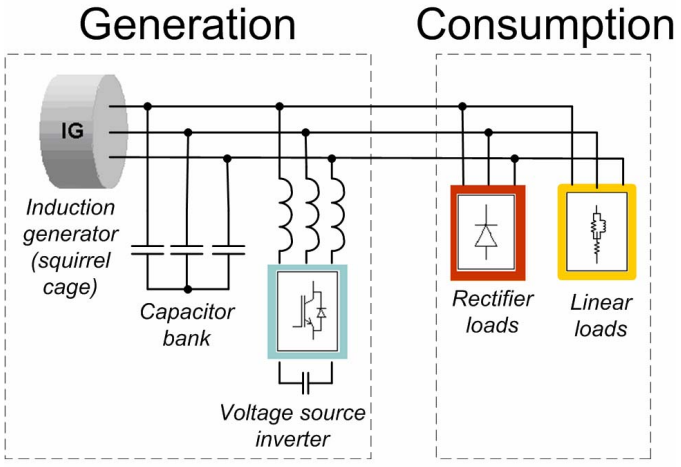

Fig. 1. A small isolated power system.

This work was partially supported through a European Community Marie Curie Fellowship and in the framework of the CTS, contract number: HPMT-CT-2001-00278.

V. Spitsa is with the Department of Electrical Engineering, Technion – Israel Institute of Technology, Haifa 32000, Israel (e-mail: spitsv1@tx.technion.ac.il).

A. Kuperman and R. Rabinovici are with the Department of Electrical Engineering, Ben-Gurion University in the Negev, Beer-Sheva 84105, Israel (e-mail: alonk@ee.bgu.ac.il, rr@ee.bgu.ac.il).

G.Weiss is with the Department of Electrical and Electronic Engineering, Imperial College of Science, Technology and Medicine, London SW7 2AZ, United Kingdom (e-mail: g.weiss@imperial.ac.uk).

II. A State-space model of the system

A control system of the induction generator and its loads consists of two loops. The external loop is based on vector control of the induction generator and its aim is to provide a constant amplitude, variable frequency three-phase voltage reference signal. The internal feedback loop achieves voltage tracking. In this paper we present only the voltage tracking controller. There are three identical inverters, each with its own LC filter and voltage controller, and we shall regard only one such inverter. Assuming for simplicity that the loads are balanced, each inverter and its load may be represented as in Fig. 2. This figure shows the load connected between one phase and the neutral line. In reality, the load has no neutral line, but for a balanced load this is an equivalent representation.

In this section a state-pace model of the electrical system in Fig. 2 is derived. Assuming that the PWM block operates without entering saturation, i.e. $|u(t)| < \frac{V_{DC}}{2}$, an average voltage approach can be applied. According to this approach the average output voltage of the inverter bridge u_f is equal to the PWM reference voltage u. We introduce the state vector, the input vector and the output vector by

$$x = \begin{bmatrix} i_1 \\ i_2 \\ V_c \end{bmatrix}, \quad \begin{bmatrix} w \\ \hline u \end{bmatrix} = \begin{bmatrix} i_g - i_d \\ V_{ref} \\ \hline u \end{bmatrix} \quad y = \begin{bmatrix} e \\ \hline i_S \end{bmatrix} \tag{1}$$

where i_1, i_2 are the currents in the inductor L_f and L respectively,

V_c is a voltage on the capacitor C,

i_g is a generator current,

i_d is a non-linear load current,

V_{ref} is the reference voltage,

u is the control input to the PWM inverter,

e is the voltage tracking error, $e = V_{ref} - V_c$,

i_s is the output current of the PWM inverter, after its LC filter.

The state space equations of the system are

$$\frac{dx}{dt} = Ax + \begin{bmatrix} B_1 & B_2 \end{bmatrix} \cdot \begin{bmatrix} w \\ \hline u \end{bmatrix}$$
$$y = \begin{bmatrix} e \\ \hline i_s \end{bmatrix} = \begin{bmatrix} C_1 \\ \hline C_2 \end{bmatrix} x + \begin{bmatrix} D_{11} & | & D_{12} \\ \hline D_{21} & | & D_{22} \end{bmatrix} \cdot \begin{bmatrix} w \\ \hline u \end{bmatrix} \tag{2}$$

where

$$A = \begin{bmatrix} -\frac{r_f R_f}{L_f(R_f + r_f)} & 0 & -\frac{r_f}{L_f(R_f + r_f)} \\ 0 & -\frac{rR}{L(R+r)} & \frac{r}{L(R+r)} \\ \frac{r_f}{C(R_f + r_f)} & -\frac{r}{C(R+r)} & -\frac{1}{C}\left[\frac{1}{(R_f + r_f)} + \frac{1}{(R+r)}\right] \end{bmatrix} \tag{3}$$

$$\begin{bmatrix} B_1 & B_2 \end{bmatrix} = \begin{bmatrix} 0 & 0 & | & \frac{r_f}{L_f(R_f + r_f)} \\ 0 & 0 & | & 0 \\ \frac{1}{C} & 0 & | & \frac{1}{C(R_f + r_f)} \end{bmatrix}, \tag{4}$$

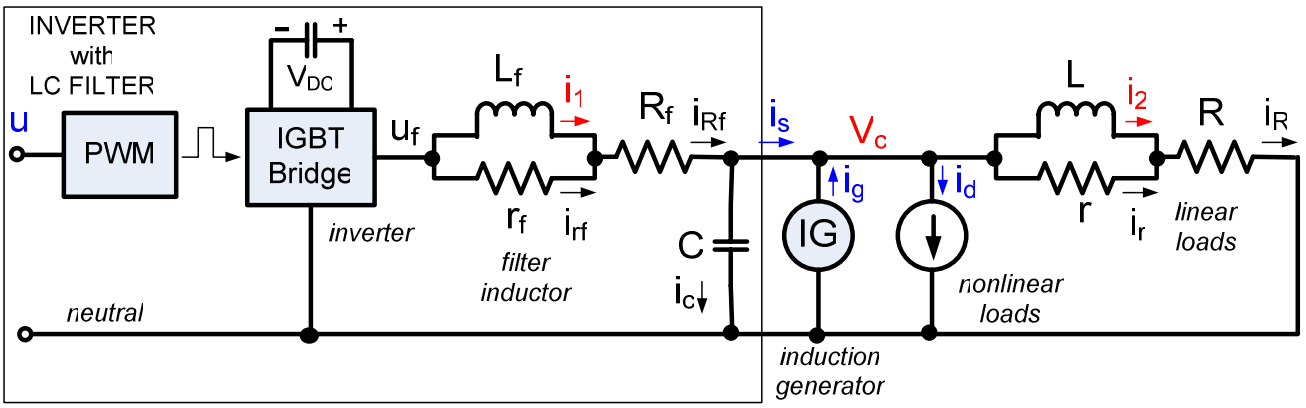

Fig. 2. A single-phase representation of the electrical system.

$$\begin{bmatrix} C_1 \\ C_2 \end{bmatrix} = \begin{bmatrix} \dfrac{0}{----} & \dfrac{0}{----} & \dfrac{-1}{----} \\ 0 & \dfrac{r}{(R+r)} & \dfrac{1}{(R+r)} \end{bmatrix}, \tag{5}$$

$$\begin{bmatrix} D_{11} & | & D_{12} \\ \hline D_{21} & | & D_{22} \end{bmatrix} = \begin{bmatrix} \dfrac{0}{----} & \dfrac{1}{----} & | & 0 \\ -1 & 0 & | & 0 \end{bmatrix}. \tag{6}$$

III. PROBLEM FORMULATION

The voltage tracking controller to be designed should achieve a very small steady-state error for any constant (possibly nonlinear) load within a reasonable range. The harmonics introduced by the nonlinear load are represented in Fig. 2 by the disturbance current i_d, which is periodic with the same period as that of the output voltage V_C. The design will be reduced to the solution of a standard H^∞ problem, similarly as in [5]. The block diagram of the control system is given in Fig. 3.

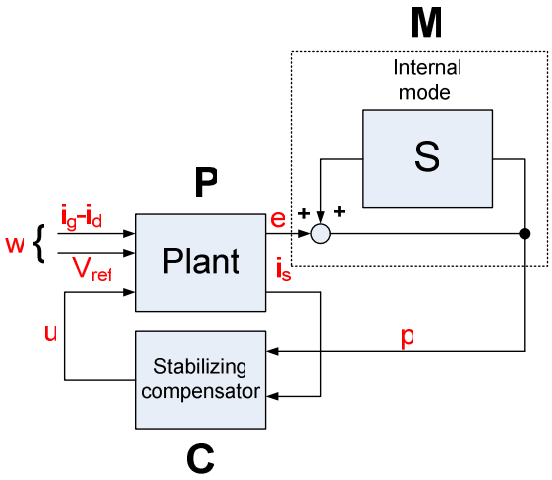

Fig. 3. Voltage tracking system.

To improve performance, an additional measurement information from the plant, i_s is supplied to the controller. The controller consists of two blocks: an internal model M and a stabilizing compensator C. under the assumption that the generator current i_g, the disturbance current i_d and the reference voltage V_{ref} are periodic with the same fundamental frequency ω_1, we propose to use the following internal model:

$$\mathbf{M}(s) = 1 + \sum_{k=1}^{N} \frac{a_k s}{s^2 + \left(k \cdot \omega_1\right)^2} = \frac{1}{1 - \mathbf{S}(s)}, \tag{7}$$

where $a_k > 0$ is the gain defining the response speed of the k-th resonant filter.

Note that we have $\mathrm{Re}\left[\mathbf{M}(s)\right] \geq 1$ for all complex s with $\mathrm{Re}\, s \geq 0$, which implies that we can represent $\mathbf{M}(s)$ as in the second part of (7), with $\|\mathbf{S}\|_\infty \leq 1$.

In our specific case, we want to ensure a very small voltage tracking error at the frequencies ω_1, $5\omega_1$ and $7\omega_1$. Indeed, errors at the harmonic frequencies 0, $3\omega_1$, $6\omega_1$, … are not important, because currents of these frequencies can not flow to the load or to the generator, due to the absence of a neutral line. Errors at even multiples of ω_1 are assumed to be negligible due to a symmetric behavior of the load with respect to a change of sign. It should be noted that ω_1 is variable and it is controlled by the external feedback loop, which is not treated in this paper. The variations of ω_1 are assumed to be slow compared to the variations of the voltages, and in our analysis of the internal control loop we assume that ω_1 is constant and unknown (but within a known range).

As mentioned, the second block of the voltage controller is the stabilizing compensator C. It has to assure the stability of the entire system forcing the error signal e to converge to a small steady-state value, similarly to the theory presented in [6]. This is achieved by the following reasoning.

According to the small gain theorem [7], if $\mathbf{T}$ and $\mathbf{S}$ are transfer functions of stable LTI systems, then the closed loop system shown in Fig. 4 remains stable if

$$\|\mathbf{ST}\|_\infty < 1. \tag{8}$$

If $\mathbf{W}$ is a stable transfer function that satisfies

$$\left|\mathbf{W}(j\omega)\right| \geq \left|\mathbf{S}(j\omega)\right| \text{ for all } \omega \in \mathbf{R}, \tag{9}$$

$$\|\mathbf{WT}\|_\infty < 1, \tag{10}$$

then (8) follows (because $\|\mathbf{S}\|_\infty \leq 1$).

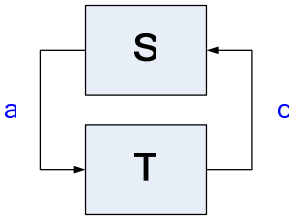

Fig. 4. A stable feedback system, an illustration for the small gain theorem.

In our case $\mathbf{T}$ represents an interconnection of the plant and the stabilizing compensator when all the external signals are zero, as shown in Fig. 5.

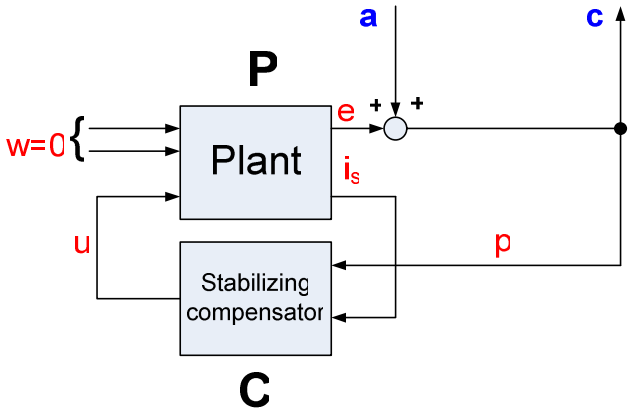

Fig. 5. The subsystem with transfer function $\mathbf{T}$ (from a to c).

First of all, a standard H^∞ control problem for the augmented plant $\tilde{\mathbf{P}}$ shown in Fig. 6 be solved. In terms Laplace transforms the system in Fig. 6 can be described by

$$\begin{bmatrix} \tilde{z} \\ \tilde{y} \end{bmatrix} = \tilde{\mathbf{P}} \begin{bmatrix} \tilde{w} \\ \tilde{y} \end{bmatrix}, \quad u = \mathbf{C}\,\tilde{y} \tag{11}$$

where (as computed in [8])

$$\tilde{\mathbf{P}} = \left[\begin{array}{ccc|ccc|c} A & 0 & 0 & 0 & 0 & B_1 & B_2 \\ B_w C_1 & A_w & 0 & B_w \xi & 0 & B_w D_{11} & B_w D_{12} \\ 0 & 0 & A_u & 0 & 0 & 0 & B_u \\ \hline 0 & C_w & 0 & 0 & 0 & 0 & 0 \\ 0 & 0 & C_u & 0 & 0 & 0 & D_u \\ \hdashline C_1 & 0 & 0 & \xi & 0 & D_{11} & D_{12} \\ C_2 & 0 & 0 & 0 & \mu & D_{21} & D_{22} \end{array}\right]. \tag{12}$$

In (12), ξ and μ are nonzero parameters giving additional freedom in the design. Moreover, the parameter μ is needed to satisfy a rank condition needed to make the H^∞ control problem solvable. The weighting high-pass transfer function

$$\mathbf{W}_u = \left[\begin{array}{c|c} A_u & B_u \\ \hline C_u & D_u \end{array}\right], \quad D_u \neq 0 \tag{13}$$

is introduced to reduce the controller gains at high frequencies.

The transfer function $\mathbf{W}$ described earlier can be chosen as a low-pass filter:

$$\mathbf{W} = \left[\begin{array}{c|c} A_w & B_w \\ \hline C_w & 0 \end{array}\right]. \tag{14}$$

To minimize the order of the stabilizing compensator, the weighting transfer functions $\mathbf{W}_u$ and $\mathbf{W}$ are chosen to be of first order.

Using the Robust Control Toolbox from MATLAB®, the central sub-optimal controller can be found for a given H^∞ norm γ_s of the transfer matrix $\mathbf{T}_{\tilde{z}\tilde{w}}$ from $\tilde{w}$ to $\tilde{z}$ as

$$\mathbf{C} = \left[\begin{array}{c|cc} A_c & B_{c1} & B_{c2} \\ \hline C_c & 0 & 0 \end{array}\right] \tag{15}$$

and $\mathbf{T}_{\tilde{z}\tilde{w}} = \mathcal{F}_l\left(\tilde{\mathbf{P}}, \mathbf{C}\right)$ where $\mathcal{F}_l$ stands for the lower fractional transformation, see [8].

According to the small gain theorem [7], the voltage tracking system shown in Fig. 3 will be stable if the closed-loop system in Fig. 6 is stable and the condition (10) holds.

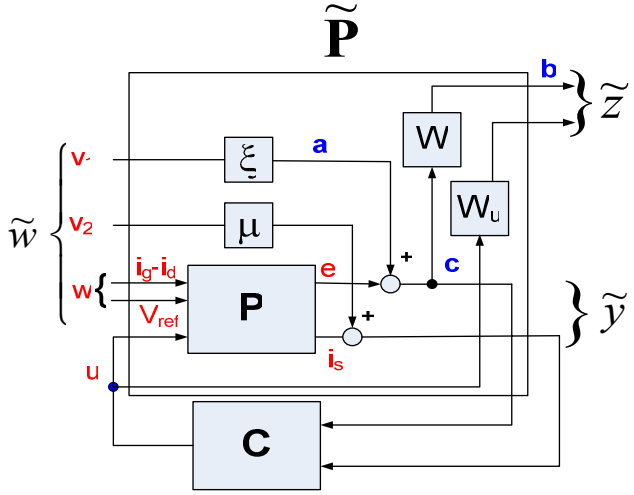

Fig. 6. Our standard H^∞ control problem.

The state space representation of the transfer function $\mathbf{WT}$ is derived in [5] and it is

$$\mathbf{WT} = \left[\begin{array}{ccc|c} A & B_2 C_c & 0 & 0 \\ B_{c1} C_1 + B_{c2} C_2 & A_c + (B_{c1} D_{12} + B_{c2} D_{22}) C_c & 0 & B_{c1} \\ B_w C_1 & B_w D_{12} C_c & A_w & B_w \\ \hline 0 & 0 & C_w & 0 \end{array}\right] \tag{16}$$

We denote

$$\gamma = \left\| \mathbf{WT} \right\|_\infty \tag{17}$$

According to (10), the additional requirement $\gamma < 1$ is imposed on the compensator. Moreover, according to a computation similar to the one in [6], an upper bound on the steady-state tracking error of the control system is

$$\left\| e_{ss} \right\|_{L^2[0,\tau]} \le 2\frac{\gamma_0}{1-\gamma} \left\| w \right\|_{L^2[0,\tau]} \tag{18}$$

where $\tau = \dfrac{2\pi}{\omega_1}$ is the fundamental period and $\gamma_0 = \left\| \mathbf{T}_{ew} \right\|_\infty$, where $\mathbf{T}_{ew}$ is the transfer function from w to e in Fig. 6. According to [5]

$$\mathbf{T}_{ew} = \left[\begin{array}{cc|c} A & B_2C_c & B_1 \\ B_{c1}C_1 + B_{c2}C_2 & A_c + \left(B_{c1}D_{12} + B_{c2}D_{22}\right)C_c & B_{c1}D_{11} + B_{c2}D_{21} \\ \hline C_1 & D_{12}C_c & D_{11} \end{array}\right] \tag{19}$$

Thus, our design objectives for the stabilizing compensator $\mathbf{C}$ are listed below:

1. $\left\| \mathbf{T}_{\tilde{z}\tilde{w}} \right\| < \gamma_s$ where γ_s is a given value of H^∞ norm.
2. $\left\| \mathbf{WT} \right\| = \gamma < 1$.
3. $\dfrac{\gamma_0}{1-\gamma} = \dfrac{\left\| \mathbf{T}_{ew} \right\|}{1-\left\| \mathbf{WT} \right\|}$ should be as small as possible.

A proposed design technique is described in the following section.

IV. OPTIMIZATION USING A GENETIC ALGORITHM

In order to solve the controller design problem as formulated in the previous section, we should choose values for the design parameters ξ, μ and the coefficients of the first-order filters $\mathbf{W}$ and $\mathbf{W}_u$, and then find the controller $\mathbf{C}$ by solving H^∞ control problem described in Section III. Then, we vary the parameters and repeat the procedure until a certain objective function nearly minimized. We define the function by

$$Q = \frac{\gamma_0}{1-\gamma} + p_{ab} + p_f \tag{20}$$

which takes into account the three design objectives at the end of the last section. Here, $p_{ab} = 0$ if $\gamma < 1$ and a very large number if $\gamma \ge 1$; p_f is a penalty term which is large if the controller gain is large at high frequencies (we omit the precise definition of p_f).

The minimization of the non-linear function Q from (20) with respect to the design parameters is a non-convex problem. Therefore, we have used a floating-point genetic algorithm [9], [10] to solve this problem.
The design procedure can be summarized as follows:

1. Solution procedure of the H^∞ problem for $\mathbf{T}_{\tilde{z}\tilde{w}} = \mathcal{F}_\ell\left(\tilde{\mathbf{P}}, \mathbf{C}\right)$ is based on the γ-iteration technique. In order to obtain the lowest admissible value of γ for which the design specifications are satisfied, we use a bisection algorithm. Using this algorithm, we determine a lower bound of the γ-iteration interval γ_{lower}, for which the design specifications are satisfied. For this purpose, initially the lower bound is assumed to lie in the interval $\left[l^0, u^0\right]$ where $l^0 = 0$ and $1 << u^0 < \gamma_{upper}$ with γ_{upper} being the upper bound of the γ-iteration interval.
2. The mid-point of the possible γ_{lower} interval is calculated $\gamma_{lower}^k = \dfrac{l^k + u^k}{2}$.
3. A large number is assigned as an initial value of the objective function Q.
4. N random parameter vectors are created.
5. For each parameter vector, the standard H^∞ problem for $\mathbf{T}_{\tilde{z}\tilde{w}}$ is solved with γ being in the interval $\left[\gamma_{lower}^k, \gamma_{upper}\right]$.
6. The objective function is evaluated with each controller calculated in the previous step to obtain an initial population.
7. The genetic algorithm starts from the initial population. It moves from generation to generation, selecting and reproducing parents with crossover and mutation operations in order to find the optimal solution according to [7]. The algorithm is terminated when a stopping criterion is met. This criterion can be specified, for example, as a maximum number of generations or population convergence.
8. The obtained value of the objective function Q is compared with the initial one assigned in Step 2. If it is smaller than the initial value than the new interval for γ_{lower} search is $\left[l^{k+1}, u^{k+1}\right] = \left[l^k, \gamma_{lower}^k\right]$ otherwise $\left[l^{k+1}, u^{k+1}\right] = \left[\gamma_{lower}^k, u^k\right]$, and the iterative procedure including steps 3-7 continues until the termination condition $u^{k+1} - l^{k=1} < \Delta_{\min}$ is satisfied with $\Delta_{\min}$ being a small number.

V. SIMULATION RESULTS

Using the design method described earlier, a sub-optimal controller has been obtained for the set of the system parameters given in Table I. Bode plots of the stabilizing compensator are presented in Figs. 7 and 8.

TABLE I
PARAMETERS OF THE AUTONOMOUS ELECTRICAL SYSTEM

Parameter	Value
$R_f, [\Omega]$	0.05
$r_f, [\Omega]$	10^{10}
$L_f, [mH]$	5
$R, [\Omega]$	100
$r, [\Omega]$	500
$L, [mH]$	0.05
$C, [\mu F]$	101.6

To examine the performance of the designed controller, it was incorporated in the full model of the autonomous power system where the induction generator is modeled as described in [11] and the non-linear rectifier load id modeled as in [12]. We incorporated an external control loop (not described here in detail), as mentioned at the beginning of Section II. The results of the simulations are presented in Figs. 9 - 12. In the first simulation, the signal V_{ref} generated by the external control loop is applied straight as the input u of PWM block.

In the second simulation, the voltage is controlled as shown in Fig. 3. As it can be seen in Figs. 9 and 10, application of the new controller significantly reduces level of the harmonic distortion. Indeed, without controller, THD of the voltage in Fig. 9 is 6.57% that violates limit recommended by IEEE 519-1992. At the same time, when the designed controller has been introduced, THD of the generator voltage reduces to 0.18% (See Fig. 10).

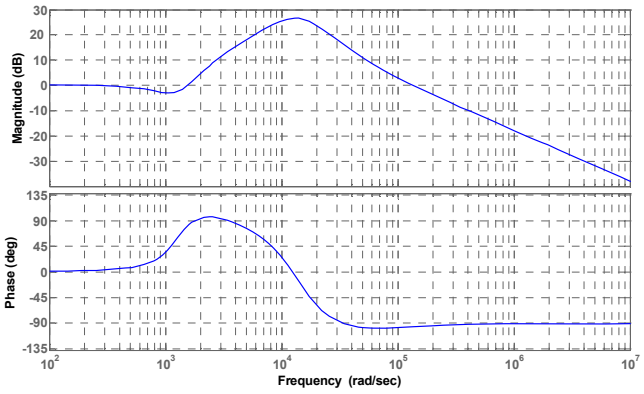

Fig. 7. Bode plot of the component C_1 of the stabilizing compensator.

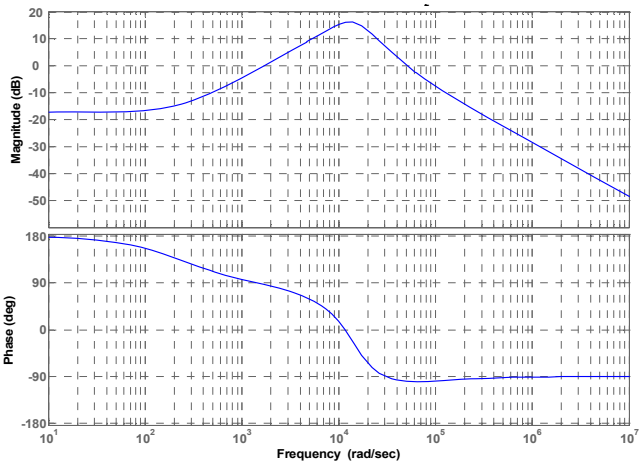

Fig. 8. Bode plot of the component C_2 of the stabilizing compensator.

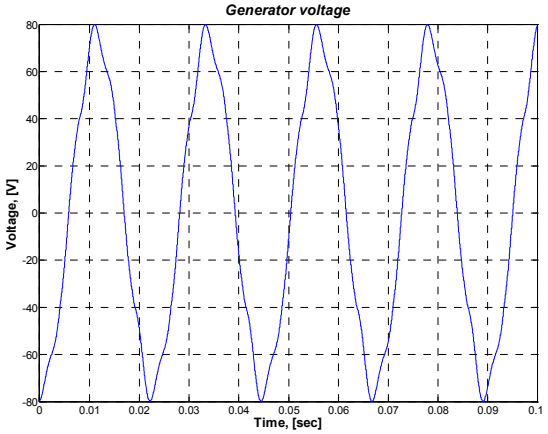

Fig. 9. Voltage waveform when the generator is not equipped with the voltage tracking controller.

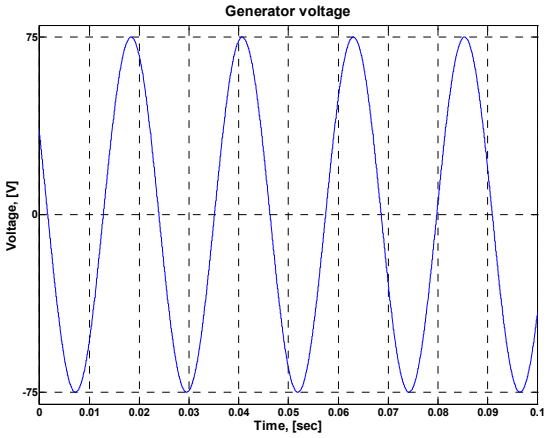

Fig. 10. Voltage waveform when the generator is equipped with the voltage tracking controller.

Analyzing the voltage tracking errors presented in Figs. 11 and 12 one may conclude that the new controller enhance steady-state tracking capabilities, especially when harmonic distortion is present: In these figures the non-linear load has been connected at time instant equal to 4 sec resulting in a maximum tracking error of 7.8 V without the controller and only 0.5 V with the controller. At the same time transient characteristics of the system have not been significantly affected by the controller.

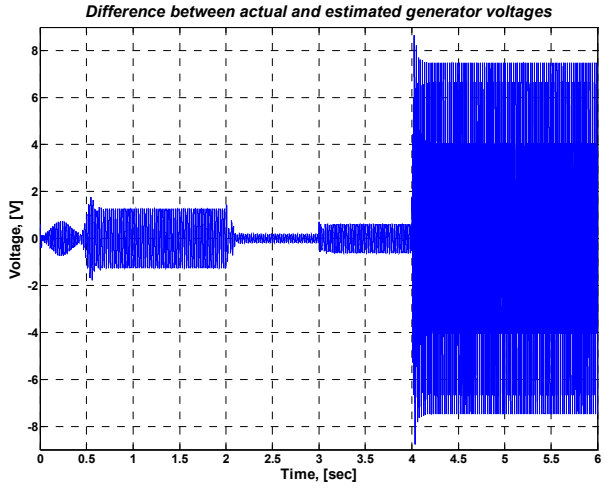

Fig. 11. Voltage tracking error without the voltage controller.

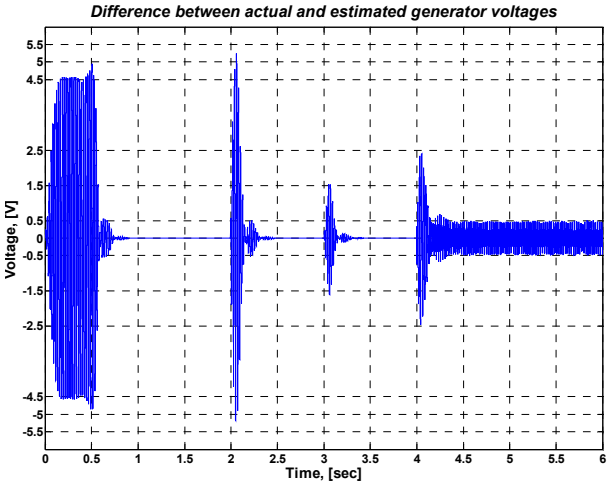

Fig. 12. Voltage tracking error with the voltage controller.

VI. CONCLUSION

In the present work the voltage controller with the adjustable finite-dimensional internal model has been designed for the autonomous power system supplied from induction generator. The design technique is based on the H^{∞} theory and incorporates a solution of the non-convex optimization problem using the float-point genetic algorithm to determine sub-optimal controller satisfying additional frequency domain specifications. It was shown that the application of the designed controller allows one to achieve a significantly better system performance than that achievable using traditional PI-controllers. This fact is due to a strong harmonic rejection executed by the new controller. Thus, the designed controller solves simultaneously two problems: voltage control at the induction generator terminals and improvement of power quality in autonomous power systems without requirements for additional equipment. The proposed solution leads to reduction of the additional power losses in electrical installations, prevents malfunction of semiconductor devices and improves performance of the electrical machines in the isolated power systems. Implementation of the designed controller using DSP can be performed using synchronous sampling.

VII. REFERENCES

[1] Muller S. Deicke M. and De Doncker R.W., *"Dobly fed induction generator systems for wind turbines"*, IEEE Industry Application Magazine, Vol. 8, no. 3, May-June 2002, pp. 26-33.

[2] Wang L. and Su J. E., *"Effects of long-shunt and short-shunt connections on voltage variations of a self-excited induction generator"*, IEEE Trans. On Energy Conversion, Vol. 12, no. 4, June 1997, pp. 368-374.

[3] Bhim Singh and Shirpakar L.B., *"Analysis of a novel solid state voltage regulator for a self-excited induction generator"*, IEE Proc. On Generation Transmission and Distribution, Vol. 145, No. 6, November 1998, pp. 647-655.

[4] Kuo S.-C. and Wang L., *"Analysis of voltage control for self-excited induction generator using a current-controlled voltage source inverter (CC-VSI)"*, IEE Proc. On Generation Transmission and Distribution, Vol. 148, No. 5, September 2001, pp. 431-437.

[5] Weiss G., Qing-Chang Zhong, Green T. C. and Jun Liang, "*H^{∞} Repetitive Control of DC-AC Converters in Microgrids*", IEEE Trans. On Power Electronics, Vol. 19, No. 1, January 2004, pp. 219- 230.

[6] Weiss G. and Hafele M., "*Repetitive Control of MIMO Systems Using H^{∞} Design*", Automatica, Vol. 35, No. 7, July 1999, pp. 1185-1199.

[7] Bhattacharyya S. P., Chapellat H. and Keel L. H., Robust Control: The Parametric Approach, Prentice Hall, New York, 1999.

[8] Green M and Limebeer D. J. N.., Robust Linear Control, Prentice-Hall, Englewood Cliffs, 1995.

[9] Michalewicz Z., Genetic Algorithms + Data Structures = Evolution Programs, AI Series, Springer-Verlag, New York, 1994.

[10] Houck C., Joines J. and Kay M., "*A Genetic Algorithm for Function Optimization: A MATLAB Implementation*", NCSU-IE TR 95-09, 1995.
Available at http://www.ie.ncsu.edu/mirage/GAToolBox/gaot/

[11] Vas P., Electrical Machines and Drives, Oxford University Press, New York, 1992.

[12] Marques G. D., "*Numerical simulation method for the slip power recovery*", IEE Proc.-Electr. Power Appl., Vol. 146, No. 1, January 1999, pp. 17-24.